Design and Flight Test of 35-GigaHertz Radar for Terrain and Obstacle Avoidance

Richard E. Zelenka*
NASA Ames Research Center,
Moffett Field, California 94035
and
Larry D. Almsted†
Honeywell Military Avionics,
Minneapolis, Minnesota 55413

I. Introduction

COLLISION avoidance is of concern to all aircraft, requiring the detection of hazardous terrain or obstacles in sufficient time for clearance maneuvers. To augment the pilot's visual collision avoidance abilities, some aircraft are equipped with enhanced-vision systems or terrain collision warning systems. Enhanced-vision systems typically project raw images from infrared or radar sensors, and can require a high degree of pilot interpretation and attention. Sensor image display systems have proven beneficial during certain flight operations, particularly during terminal operations.[1] However, such raw sensor display presentations are limited during more aggressive flight profiles, where the lack of display memory requires the constant redetection of hazards to the aircraft. Stored map derived terrain collision warning systems, such as those commonly termed controlled flight into terrain (CFIT) warning systems,[2,3] do not identify hazards placed after map sampling and can suffer from severe vertical elevation mapping errors.[4,5] The collision avoidance requirement is even more demanding for helicopters, as their unique capabilities result in extensive operations at low-altitude, near-to-terrain, and hazardous obstacles.

In this work, a scanning, pencil-beam millimeter wave (MMW) radar forward sensor is used to determine whether an aircraft's flight path is clear of obstructions. The three-dimensional radar's returns are used to construct a terrain and obstacle database surrounding the aircraft, which is presented to the pilot as a synthetic perspective display. The 35-GHz MMW band allows operations in degraded weather (e.g., rain, fog) with narrow beam shapes and small antennas. The radar-derived high-resolution, high-accuracy database could also be used to drive aircraft guidance trajectories.[6] The synthetic perspective display would be of greatest benefit during degraded weather operations, or flight in unfamiliar areas, such as those of emergency medical service (EMS), search and rescue, and airborne firefighting. This Note presents the design and flight test results of a 35-GHz radar and associated pilot display. Through flight test, the radar/display system demonstrated its potential usefulness for terrain and obstacle collision avoidance.

II. MMW Radar System Description

A block diagram of the Honeywell/NASA 35-GHz biphase-modulated, coherent-pulsed millimeter wave radar system is provided as Fig. 1. The system takes advantage of existing 4.3-GHz radar altimeter components in performing the transmit and receiving functions. The 4.3-GHz signal is passed through an upconverter to 35 GHz and emitted as a scanning, pencil-beam through a twist-reflector-type antenna and circularly polarized lens. Radar returns are down-converted to 4.3 GHz and processed using the 4.3-GHz radar altimeter components. The use of 35 GHz affords good weather penetration capability, scattering at low grazing angles, and the use of a small antenna (9 in. diam). The complete set of externally mounted components weigh ~31 lb and are contained in a ~20 in. long by 12 in. diam cylindrical assembly. Because of the heavy reliance on existing radar altimeter components, the system is expected to yield a low-cost, highly reliable radar system.

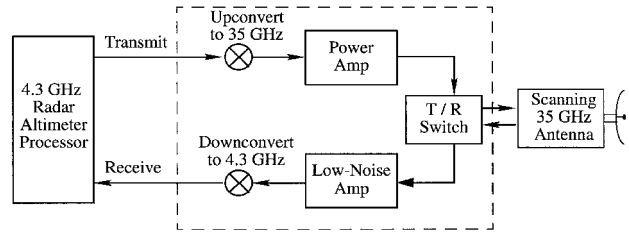

Fig. 1 Forward looking 35-GHz radar block diagram.

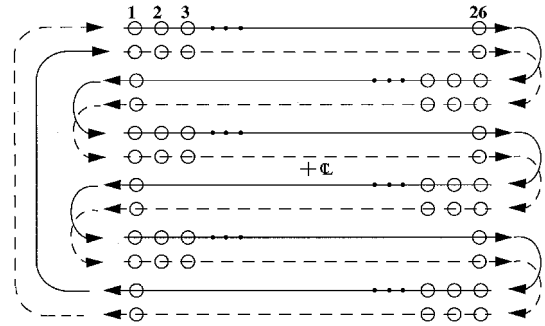

Fig. 2 Fully interlaced 20 by 50 deg radar scan.

The 2.6-deg pencil-beams (3 dB) are scanned to cover a 20-deg elevation by 50-deg azimuth field of view (FOV) in 1 s, fully interlaced in 2 s. Range gating varies from 16 to 32 ft over the 96–1056 ft range of the radar. The first 20 gates, from 96 to 416 ft, are of 16-ft size. Ranges from 416 to 1056 ft are of 32-ft size. The radar system was designed to allow easy growth in range to 10,000 ft. The antenna scan pattern and interlaced characteristics are provided in Fig. 2. An early single-beam, nonscanning version of this radar demonstrated excellent correlation between predicted and flight test performance.[7]

III. Terrain/Obstacle Database Construction

The valid detections output from the MMW radar are received as sensor-referenced range, azimuth, and elevation (or ρ, θ, ϕ) and transformed to inertial (x, y, z) using the aircraft state information supplied by the aircraft navigation system. These detections are used to create and update the three-dimensional terrain/obstruction database (TOD). The terrain and obstacles located by the radar forward sensor are stored in an inertially referenced grid system with grid resolution of 20 ft. The area considered by the guidance system is 2500 ft^2 and is periodically shifted through the grid system such that its center position remains approximately below the aircraft. The grid is initialized using the difference in the aircraft's current mean sea level (MSL) altitude minus the radar altimeter above ground level (AGL) altitude.

Several approaches to blending of multiple sensor returns in constructing the terrain/obstacle database were considered. The

Received Oct. 5, 1996; presented as Paper 96-5617 at the 1st World Aviation Congress, Los Angeles, CA, Oct. 22–24, 1996; revision received Nov. 19, 1996; accepted for publication Nov. 19, 1996.

*Group Leader, Flight Deck Branch, M/S 210-9. Senior Member AIAA.

†Engineering Manager, 2600 Ridgway Parkway.

fundamental tradeoff is to develop a processing scheme that will perform adequate noise rejection while maintaining elevation sensitivity in each grid. This is especially difficult and important for storing obstacles where two distinct elevation values exist at the same inertial location (i.e., a pole or tower and the ground below it). Techniques implemented in flight tests were the maximum likelihood approach and the simple setting of the grid elevations to the maximum elevation value found for each grid. In both techniques, one TOD cell was updated per radar return for near ranges, with an additional adjacent eight cells updated for far ranges. The crossover between one and multiple TOD cell updating for a given radar return was set by the range at which the beam spread exceeded one TOD cell width. For our setting of TOD cells to 20 ft, this value occurred at 440 ft.

The maximum likelihood algorithm calculates the elevation value for a particular grid, which maximizes the probability of the elevation measurements to that grid, taking in statistical properties of the measurements known a priori. This method has the advantage of drawing on all measurements recorded for a given grid cell, allowing prior measurements to statistically influence the elevation estimates.

The error in the vertical elevation measurement from a given radar beam is the result of the combined errors from the radar beam width (cross-track error) and range gating (along-track error). Each of these errors is modeled as a uniform distribution, reflecting the equally likely probability of a detected target residing anywhere within the declared range bin, and the equally likely probability of residing within the beam 3 dB spread of 2.6 deg. Although it is possible for certain strong targets to lie outside the beam spread and still result in a radar detection, such occurrences are considered rare.

For a given range ρ_0 and radar beam angle from horizontal η_0, the uniform zero-mean probability distribution widths are

$$a = 2\rho_0 \cos \eta_0 \tan(1.3 \text{ deg})$$

caused by beam width, and

$$b = 16 \sin \eta_0, \quad \text{for} \quad 96 \leq \rho_0 \leq 416$$

$$= 32 \sin \eta_0, \quad \text{for} \quad 416 < \rho_0 \leq 1056$$

caused by range gating.

The combined probability distribution in the vertical dimension is found as the sum of these two uniform distributions. The result is a flat-topped triangular probability distribution, with breakpoint at $\pm|a - b|$. Matching areas of this probability distribution with that of the Gaussian distribution at this breakpoint iteratively yields a normal distribution and associated standard deviation. This σ_{radar} value can then be used to combine measurements through the maximum likelihood estimate.[8] Considering the elevation of each TOD cell as a state to be estimated

$$z_{\text{update}} = \frac{\sigma^2_{\text{radar}} \cdot z_{\text{existing}} + \sigma^2_{\text{existing}} \cdot z_{\text{radar}}}{\sigma^2_{\text{radar}} + \sigma^2_{\text{existing}}}$$

$$\sigma^2_{\text{update}} = \frac{\sigma^2_{\text{radar}} \cdot \sigma^2_{\text{existing}}}{\sigma^2_{\text{radar}} + \sigma^2_{\text{existing}}}$$

IV. Pilot Display

The radar-derived TOD is presented to the pilot on a panel-mounted display as a three-dimensional synthetic perspective grid display. Each grid is drawn at the height estimated from current and prior radar returns in one of the processing techniques discussed. For engineering development, the grid perspective display could be overlaid onto a video image provided by a camera mounted adjacent to the radar.

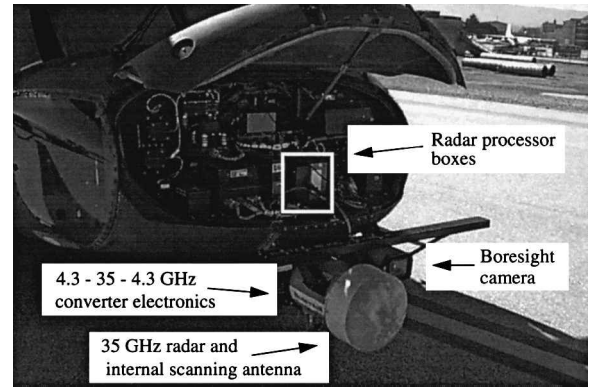

Fig. 3 UH-60 test helicopter with 35-GHz radar components.

V. Flight Test Integration

Flights were conducted aboard the NASA/Army Rotorcraft Airborne Systems Concepts Airborne Laboratory (RASCAL) UH-60 test helicopter based at NASA Ames Research Center. This research aircraft includes satellite/inertial navigation, digital data recorders for full aircraft state information (and radar outputs), panel-mounted displays in cockpit and crew area, an externally mounted color camera, and a Silicon Graphics Onyx workstation for high-fidelity graphics generation.[9] The 35-GHz radar was mounted on the nose of the aircraft on an experimental mounting bar. A camera, mounted adjacent to the radar, allowed merged video recordings of the pilot presentations of the perspective TOD display with that from the camera. Data collection included radar output, aircraft state, and pilot comments. Figure 3 shows the radar components as mounted on the test helicopter.

VI. Flight Test Results

Flights were conducted during day visual flight rules conditions in flat and moderately rugged mountainous terrain. Test profiles included flights among tower and wire obstacles. Speeds flown were between 20–60 kn, at altitudes of 200-ft AGL and below. Tests of the radar system found the radar capable of detecting low grazing angle terrain, towers, and trees without difficulty. While the radar was not designed to detect wires and cables, it detected high-tension transmission towers, and there were indications that it could intermittently detect the cables. It was assumed this occurred on multistranded cables where the reflection from the wires was diffuse rather than the more specular reflection produced from smooth wires.

The maximum likelihood algorithm approach, with a vertical obstacle threshold, was found to be a very favorable measurement processing technique for creating and updating the terrain/obstacle database from the radar returns. The alternate database construction technique, that of using the maximum value of elevation for each grid cell, was found to be somewhat noisy and disconcerting to the pilot. The maximum likelihood approach was implemented as described earlier except for a threshold bias check to account for tall, narrow pole-like obstacles. Should an elevation value for a particular radar return exceed the computed maximum likelihood elevation plus a threshold bias term (set to 30 ft), the radar return value was used and overrode the maximum likelihood computed estimate.

The three-dimensional grid–world perspective view display was able to be reliably constructed and rendered from the radar's returns, creating a fairly accurate representation of the scene surrounding the helicopter. However, the current limited range did require flights at low altitude and speed so as to not overfly the FOV and range of the sensor. Figure 4 depicts a

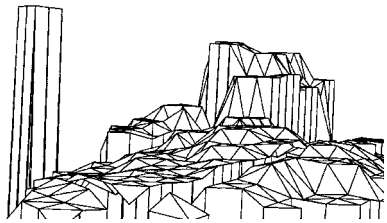

Fig. 4 Perspective grid-world display in hilly terrain with adjacent (left) tower obstacle.

representative radar-generated grid display from flight tests, in which the aircraft was heading toward a hill with an adjacent (left) tower.

VII. Concluding Remarks

1) A millimeter wave scanning, pencil-beam radar forward sensor and associated pilot display were developed for use as a collision avoidance aid. The system incorporates existing radar altimeter components in its design, to support a low-cost, highly reliable radar system.

2) The radar was integrated and flight tested aboard a UH-60 test helicopter. The radar successfully detected a variety of obstacles, building a terrain/obstacle database in real-time used to construct a synthetic view pilot display of the area surrounding the aircraft. These flight trials demonstrated the potential usefulness of the forward-looking radar/display system for terrain and obstacle collision avoidance.

References

[1]Burgess, M. A., "Synthetic Vision Technology Demonstration Final Report," DOT/FAA/RD-93/40, 1, Dec. 1993.

[2]Hewitt, C., and Broatch, S., "A Tactical Navigation and Routing System for Low-Level Flight," AGARD 2nd Mission Systems Panel Symposium on Low-Level and Nap-of-the-Earth (N.O.E.) Night Operations, Pratica di Mare (Rome, Italy), Oct. 1994, p. 11.1–11.10.

[3]Young, C. S., "Warning System Concepts to Prevent Controlled Flight into Terrain (CFIT)," *Proceedings of the IEEE/AIAA Digital Avionics Systems Conference*, Inst. of Electrical and Electronics Engineers, New York, 1993, pp. 463–468.

[4]Nordmeyer, R., "Enhanced Terrain Masked Penetration Final Technical Report," Air Force Systems Command, Air Force Wright Aeronautical Labs., TR-86-1079, Sept. 1986.

[5]Zelenka, R. E., and Swenson, H. N., "Appraisal of Digital Terrain Elevation Data for Low-Altitude Flight," *Proceedings of the American Helicopter Society 48th Annual Forum*, American Helicopter Society, Alexandria, VA, 1992, pp. 1561–1569.

[6]Zelenka, R. E., Clark, R., Zirkler, A., Saari, R., and Branigan, R., "Development and Flight Test of Terrain-Referenced Guidance with Ladar Forward Sensor," *Journal of Guidance, Control, and Dynamics*, Vol. 19, No. 4, 1996, pp. 823–828.

[7]Becker, R. C., and Almsted, L. D., "Flight Test Evaluation of a 35 GHz Forward Looking Altimeter for Terrain Avoidance," *Proceedings of the IEEE/AIAA Digital Avionics Systems Conference*, Inst. of Electrical and Electronics Engineers, New York, 1994, pp. 586–589.

[8]Kweon, I. S., and Kanade, T., "High-Resolution Terrain Map from Multiple Sensor Data," *IEEE Transactions on Pattern Analysis and Machine Intelligence*, Vol. 14, No. 2, 1992, pp. 278–292.

[9]Jacobsen, R. A., Rediess, N. A., Hindson, W. A., and Aiken, E. W., "Current and Planned Capabilities of the NASA/Army Rotorcraft Aircrew Systems Concepts Airborne Laboratory (RASCAL)," *Proceedings of the American Helicopter Society 51st Annual Forum*, American Helicopter Society, Alexandria, VA, 1995, pp. 758–771.